Methyl Groups as Probes of Structure and Dynamics in NMR Studies of High-Molecular-Weight Proteins

Vitali Tugarinov and Lewis E. Kay*[a]

Introduction

Methyl groups are of particular interest in NMR studies of proteins since they occur frequently in the hydrophobic cores of these molecules[1] and thus are often sensitive reporters of structure and dynamics. Methyl probes can play a very important role in applications that involve high-molecular-weight proteins because of favorable properties that facilitate the recording of NMR spectra with high sensitivity and resolution. First, the threefold degeneracy of methyl protons in $^{13}CH_3$ isotopomers ($^{13}CH_3$, $^{13}CH_2D$, and $^{13}CHD_2$ methyls will be considered in this review) effectively increases the concentration of each group significantly beyond that for, say, backbone amides. Second, because methyl groups are localized at the peripheries of side chains, many tend to be dynamic;[2] this leads to slower relaxation that can be exploited in studies of large systems. Third, in the past few years it has become possible to produce proteins in which methyl groups are selectively protonated in a highly deuterated background; this leads to further enhanced relaxation properties that greatly increase the size of systems that can be studied.[3] Fourth, distances between proximal methyl groups, established on the basis of NOEs, often connect regions of the molecule that are far removed in primary structure.[4–8] In addition, these moieties serve as probes in investigations of protein–ligand interactions,[9,10] fast and slow timescale side-chain dynamics,[11–16] dynamics of protein folding,[17] and in the detection of proteins and complexes in in-cell NMR experiments.[18]

In this Minireview, we focus on using methyl groups to study both structure and dynamics in high-molecular-weight proteins. A key aspect has been the interplay between new isotope-labeling methodology and NMR techniques that are specifically designed for a given labeling pattern. Thus, a description of the new labeling approaches is first presented, followed by a brief summary of the NMR experiments that have been developed for site-specific methyl assignments. The relaxation properties of methyl groups are discussed, and basic principles of methyl-TROSY spectroscopy are presented. Finally, a number of practical applications involving global protein-fold determination and studies of side-chain dynamics are described.

The approaches and concepts described here are illustrated with applications to the enzyme malate synthase G (MSG) from *E. coli*—a monomeric 723-residue protein (82 kDa)[19–21] that has been extensively characterized by NMR in our laboratory over the past several years[3] and whose global fold has been recently derived de novo from NMR data exclusively.[22] MSG is a four-domain enzyme that catalyzes the Claisen condensation of glyoxylate and acetyl-CoA to produce malate and is a part of a biosynthetic bypass ("glyoxylate shunt") that is activated in many pathogenic microorganisms under anaerobic conditions.[23] Since the glyoxylate shunt is absent in man, the enzymes of this bypass have recently been recognized as potential targets for drug design to improve existing antibiotic agents.[24–26]

α-Ketoacid Precursors for Biosynthetic Labeling of Methyl Sites

Certain α-ketoacids can serve as biosynthetic precursors of a number of methyl-bearing amino acids in proteins over-expressed in minimal media. Rosen et al. have shown that the use of [^{1}H,^{13}C]-labeled pyruvate as the main carbon source in D_2O-based minimal-media expression of proteins results in high levels of proton incorporation in methyl positions of Ala, Ile(γ2 only), Leu, and Val in an otherwise highly deuterated protein.[27] Unfortunately, because the protons of the methyl group of pyruvate exchange with solvent, proteins are produced with all four of the possible methyl isotopomers ($^{13}CH_3$, $^{13}CH_2D$, $^{13}CHD_2$, and $^{13}CD_3$), although it is possible to skew the population of methyls that are "produced" heavily toward the fully protonated variety. The isotopic "dilution" associated with the generation of $^{13}CH_3$-, $^{13}CH_2D$-, and $^{13}CHD_2$-labeled methyl groups in the same protein sample compromises the sensitivity and resolution of NMR spectra due to one-bond ^{13}C (~0.3 ppm) and small two-bond ^1H (~0.02 ppm) isotope shifts that separate the resonances of each isotopomer. As a result, this method has not become widely used for the production of protein samples for structural studies, although applications that involve the generation of fully protonated proteins with selective ^{13}C incorporation only at methyl sites for relaxation studies have emerged.[13–16,28,29]

[a] *Dr. V. Tugarinov, Prof. Dr. L. E. Kay*
Departments of Medical Genetics & Microbiology, Biochemistry and Chemistry
University of Toronto, Medical Sciences Building
1 King's College Circle, Toronto, Ontario, M5S 1A8 (Canada)
Fax: (+1) 416-978-6885
E-mail: kay@pound.med.utoronto.ca

 DOI: 10.1002/cbic.200500110

Structural studies of high-molecular-weight proteins that rely principally on methyl groups are best carried out on highly deuterated, $^{13}CH_3$-labeled molecules. Gardner and Kay[30] and later Goto et al.[31] have described robust and cost-effective labeling procedures that make use of α-ketobutyric and α-ketoisovaleric acids as biosynthetic precursors for the production of deuterated proteins with protonation restricted to the Ileδ1 and Leuδ/Valγ positions, respectively. Although the number of methyl probes is decreased relative to the pyruvate-based scheme, several important advantages are associated with this approach: i) depending on the desired labeling scheme for the rest of the protein either [D]- or [D,^{13}C]-D-glucose may be used as the primary carbon source in protein production, ii) incorporation of the desired label into Ile, Leu, and Val methyl sites is near quantitative with no scrambling, and, finally, iii) due to advances in organic synthesis, virtually any combination of ^{12}C/^{13}C and H/D can be introduced into α-ketobutyrate and α-ketoisovalerate and, therefore, into the side-chains of Ileδ1/Leuδ/Valγ in otherwise highly deuterated proteins. Scheme 1 shows the chemical formulae of a number of α-ketobutyric (**I**–**IV**) and α-ketoisovaleric (**V**–**VIII**) acids with different isotopic labels that are currently used as biosynthetic precursors in our laboratory for NMR studies of high-molecular-weight proteins. Of note, compounds **I** and **V** were used earlier by Gardner et al. in studies of maltose-binding protein (MBP, 370 residues) with selective protonation at the Ileδ1/Leuδ/Valγ sites.[32]

Several authors have described procedures for the synthesis of some of the α-ketoacid precursors shown in Scheme 1, although all compounds are now commercially available. The Abbott group has developed synthetic methods for the production of ^{13}C methyl-labeled α-ketobutyric and α-ketoisovaleric acids.[9] An alternative and more cost-effective synthetic strategy for the production of α-ketoacids with this labeling pattern by using Grignard chemistry has been described by Gross et al. for high-throughput studies of protein–ligand interactions.[10] Very recently, Konrat and co-workers reported a versatile synthetic procedure that allows the incorporation of any desired isotope pattern into α-ketobutyrate or α-ketoisovalerate with high efficiency.[33] Rather than concentrating on the details of the available synthetic strategies, we describe how each of these precursors can be utilized in NMR applications involving high-molecular-weight proteins. Typically, precursors with the desired labeling patterns are added to D_2O-based growth media approximately 1 hour prior to induction of protein over-expression, and the expression times are kept reasonably short (4–6 h) to maximize the incorporation of the desired isotope label.[31,32] A methyl ^{1}H,^{13}C correlation map of {Ileδ1(^{1}H),Leu($^{13}CH_3$,$^{12}CD_3$),Val($^{13}CH_3$,$^{12}CD_3$)} U-[^{15}N,^{13}C,D] MSG, produced by using precursors **I** and **VI** from Scheme 1 is shown in Figure 1. Similar protein samples have also been produced with a combination of compounds **III**/**IV** (for Ile) and/or **VIII** (for Leu/Val) to produce protein samples with methyls of the $^{13}CH_2D$ or $^{13}CHD_2$ variety for relaxation studies (see below), illustrated for Ile12 of MSG (Figure 1 inset). The fact that a separate protein preparation must be made for each desired isotopomer is more than compensated for by the high quality of the resulting spectra, both in terms of resolution and sensitivity.

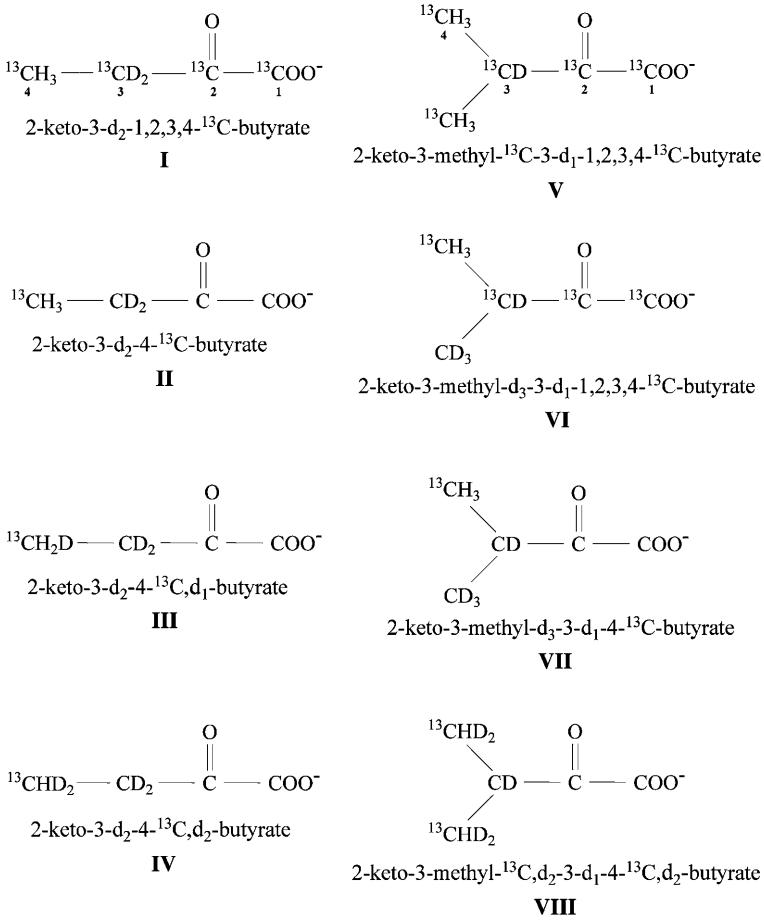

Scheme 1. Partial list of isotopically labeled α-ketoacids that are commercially available and can be used as biosynthetic precursors in the *E. coli*-based growth of methyl ^{13}C,^{1}H-labeled proteins. Sodium salts of α-ketobutyric and α-ketoisovaleric acids protonated at position 3 are available and the precursors can be quantitatively exchanged to 3-^{2}H at high pH in D_2O.[31] These precursors are added in amounts of ~50 mg (butyric acid) and ~100 mg (valeric acid) per liter of growth medium approximately 1 h prior to induction of protein over-expression.[31]

Assignment of Ileδ1/Leuδ/Valγ Methyls in High-Molecular-Weight Proteins

Methyl ^{1}H and ^{13}C assignments in MSG have been carried out on highly deuterated, methyl protonated samples produced from compounds **I** (Ileδ1-[^{1}H]) and **VI** (Leu,Val nonstereospecifically ^{13}C-enriched at a single methyl site), with uniform ^{13}C-labeling of all other sites.[34] This labeling strategy generates linear ^{13}C spin systems for Leu and Val, while Ile can effectively be linearized through the application of "selective pulses",[35] thereby avoiding problems arising from magnetization losses at the branch points of these side-chains (i.e., β(γ) in Ile, Val(Leu)]. The gains in sensitivity that ensue outweigh the losses associated with the twofold dilution of methyl groups.[34,53]

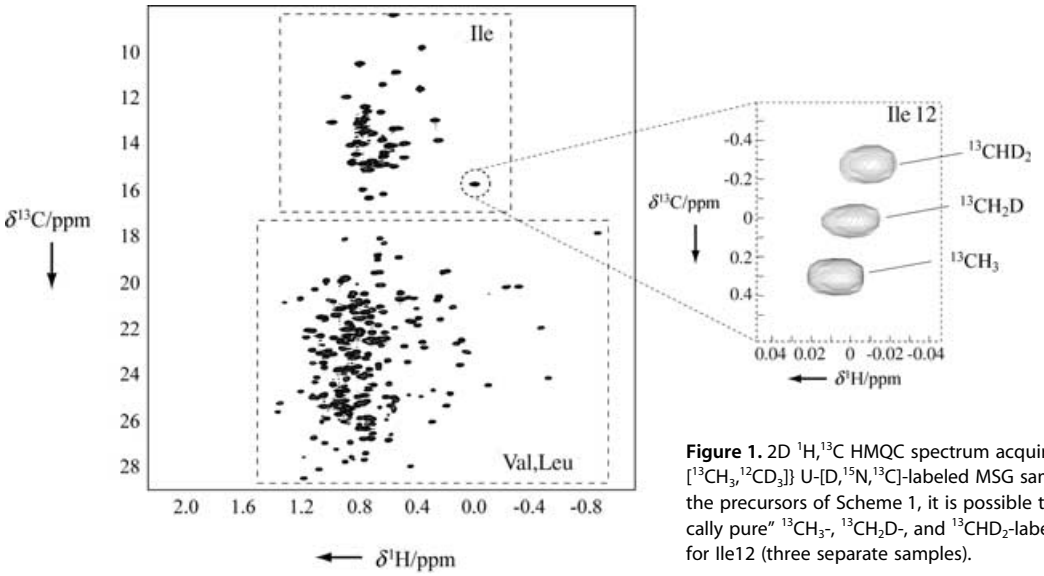

Figure 1. 2D ^{1}H,^{13}C HMQC spectrum acquired on an {Ileδ1-[$^{13}CH_3$] Leu,Val-[$^{13}CH_3$,$^{12}CD_3$]} U-[D,^{15}N,^{13}C]-labeled MSG sample (D_2O) at 800 MHz, 37 °C. With the precursors of Scheme 1, it is possible to produce samples with "isotopically pure" $^{13}CH_3$-, $^{13}CH_2D$-, and $^{13}CHD_2$-labeled methyl groups, as illustrated for Ile12 (three separate samples).

Figure 2A (top) illustrates the magnetization flow in a COSY-based HN-detected experiment in which net magnetization is transferred from the methyl group to the backbone amide, thus generating spectra containing correlations of the form [$\omega_{C_{methyl}}(i)$, $\omega_N(i)$,$\omega_{HN}(i)$] and [$\omega_{H_{methyl}}(i)$,$\omega_N(i)$,$\omega_{HN}(i)$]. Figure 2 (bottom) shows a pair of strips from data sets recorded on an {Ileδ1($^{13}CH_3$),Leu($^{13}CH_3$,$^{12}CD_3$), Val($^{13}CH_3$,$^{12}CD_3$)}, U-[^{15}N,^{13}C,D] sample of MSG (276 protonated methyls), 37 °C,[34] extracted at the amide ^{15}N chemical shift of Leu202 that has been used to assign methyl ^{13}C and ^{1}H resonances of this residue. An alternative and complimentary approach for the assignment of methyl groups is shown in Figure 2B (top) in which magnetization is transferred from methyls to aliphatic carbons in an "out-and-back" manner, thus circumventing losses associated with the net transfer to amides.[34] As with the HN-detected experiments, these schemes benefit from the Leu,Val-[$^{13}CH_3$,$^{12}CD_3$]-labeling scheme. A single 3D data set with correlations of the form [$\omega_{C_\gamma C_\beta C_\alpha}(i)$,$\omega_{C_{methyl}}(i)$,$\omega_{H_{methyl}}(i)$] for Ile and Leu, and [$\omega_{C_\beta C_\alpha}(i)$, $\omega_{C_{methyl}}(i)$,$\omega_{H_{methyl}}(i)$] for Val can be obtained, with cross peaks connecting successive aliphatic carbons alternating in phase. Additional experiments can be recorded to relay the signal to the ^{13}CO spin and back (shown with dashed arrows in Figure 2B); this provides correlations of the form [$\omega_{CO}(i)$,$\omega_{C_{methyl}}(i)$,$\omega_{H_{methyl}}(i)$]. Figure 2B (bottom) illustrates $^1H_{methyl}$–$^{13}C_{aliph}$ and $^1H_{methyl}$–^{13}CO strips from these data sets for Leu202 δ2 of MSG. The sequence-specific assignments of Ile, Leu, and Val methyls can be obtained by matching the three ^{13}C frequencies ($^{13}C_\omega$,$^{13}C_\beta$,^{13}CO) that are obtained from these experiments to those available from the compiled list of backbone and $^{13}C_\beta$ assignments. Note that, unlike in HN-detected data sets, the methyl out-and-back schemes provide

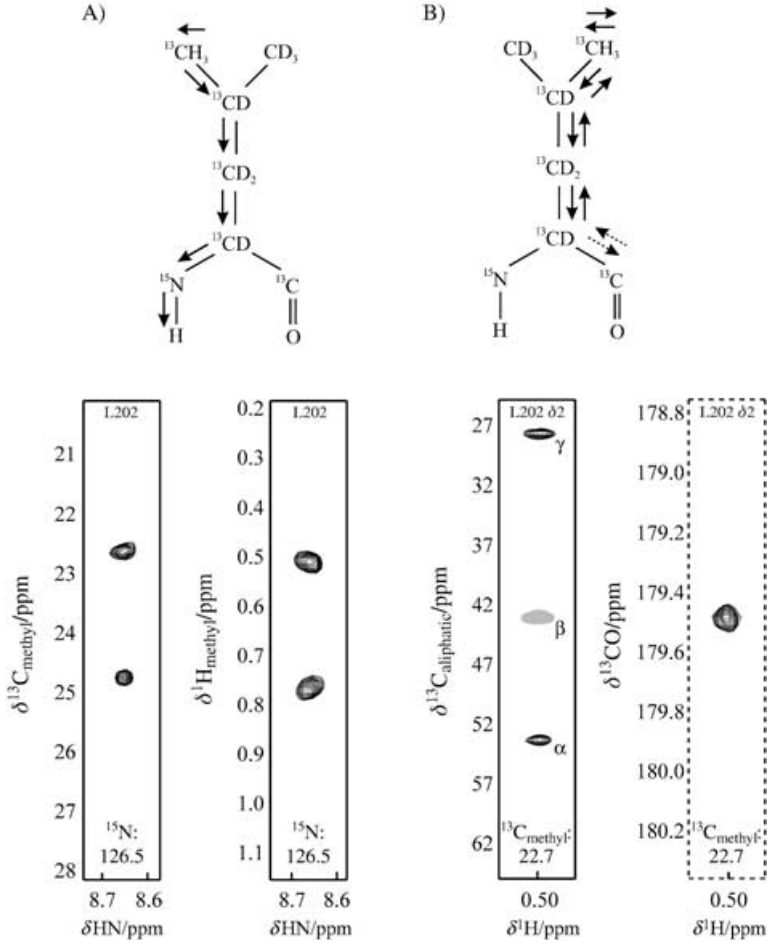

Figure 2. A) Top: Schematic diagram of the magnetization flow in $^{13}C_{methyl}$-HN experiments for assignment of Ile(δ1), Leu and Val methyl groups in high-molecular-weight proteins. Bottom: Strips from 3D HN-COSY data sets at the ^{15}N chemical shift of L202 (126.5 ppm) showing $^{13}C_{methyl}$–HN and $^1H_{methyl}$–HN correlations.[34] Spectra were recorded on an {Ileδ1-[$^{13}CH_3$] Leu,Val-[$^{13}CH_3$,$^{12}CD_3$]} U-[D,^{15}N,^{13}C]-labeled MSG sample, 37 °C. B) Top: Schematic diagram of the magnetization transfer steps in the methyl "out-and-back" experiments recorded on the same sample as in (A). Bottom: Selected $^1H_{methyl}$–$^{13}C_{aliphatic}$ and $^1H_{methyl}$–^{13}CO strips with correlations at the $^{13}C_{methyl}$ chemical shift of L202 δ2 (22.7 ppm). The negative peak ($^{13}C_\beta$) is shown in gray.

1H–^{13}C connectivities within a given methyl group de facto, thus facilitating assignment, and are significantly more sensitive (on average between five- and tenfold).[34]

Methyl-TROSY Spectroscopy

It has long been known that multiplet components associated with specific transitions in a spin system can relax at very different rates due to interference effects between relaxation interactions. This differential relaxation can be used to study molecular dynamics, an approach pioneered by Werbelow and Grant[36] and Vold and Vold.[37] Alternatively, the components that relax most slowly can be preserved by using the so-called TROSY (transverse relaxation-optimized spectroscopy) effect,[38] in which fast and slowly relaxing lines are sequestered; by focusing on magnetization-transfer pathways that derive exclusively from the long-lived transitions, significant gains in sensitivity and resolution can be obtained. The first applications of TROSY involved ^{15}N,^{1}H[38] and aromatic ^{13}C,^{1}H[39] spin systems; TROSY approaches for methyl ($^{13}CH_3$ and $^{13}CH_2D$)[40,41] and methylene ($^{13}CH_2$)[42] groups have subsequently been published.

The origin of the TROSY effect for $^{13}CH_3$ and $^{13}CH_2D$ methyl groups can be understood by considering energy-level diagrams for AX_3 [$^{13}CH_3$] and AX_2 [$^{13}CH_2D$] spin systems, Figure 3 A and B, respectively (the deuteron is treated as a "silent" spin). For completeness, the energy level diagram of an AX [$^{13}CHD_2$] spin system is also presented. Detailed calculations show that the relaxation of individual single-quantum ^{1}H (vertical lines) or ^{13}C (horizontal lines) transitions are coupled in the general case and that they depend primarily on dipolar contributions that derive from auto- and cross-correlated relaxation interactions from within the methyl group.[43–46] However, in the slow tumbling limit, $\omega_c\tau_c \gg 1$, where ω_c and τ_c correspond to the ^{13}C Larmor frequency and the overall tumbling time, respectively, and assuming that the methyl group rotates very rapidly about its threefold axis, the situation is simplified considerably, and the transitions relax in a single exponential manner.[47] The (partial) cancellation of dipolar fields leads to long-lived lines with rate constants, $R^S_{2,X}$, while the constructive addition of dipolar fields results in enhanced relaxation, $R^f_{2,X}$ (X = ^{1}H or ^{13}C).[36,47,48] For example, for Ileδ1-[$^{13}CH_3$] U-[D,^{15}N,^{12}C]-labeled MSG at 37 °C, measured values for $R^S_{2,X}$ are 26 ± 9 and 22 ± 12 s^{-1} for ^{1}H and ^{13}C, respectively, while the corresponding

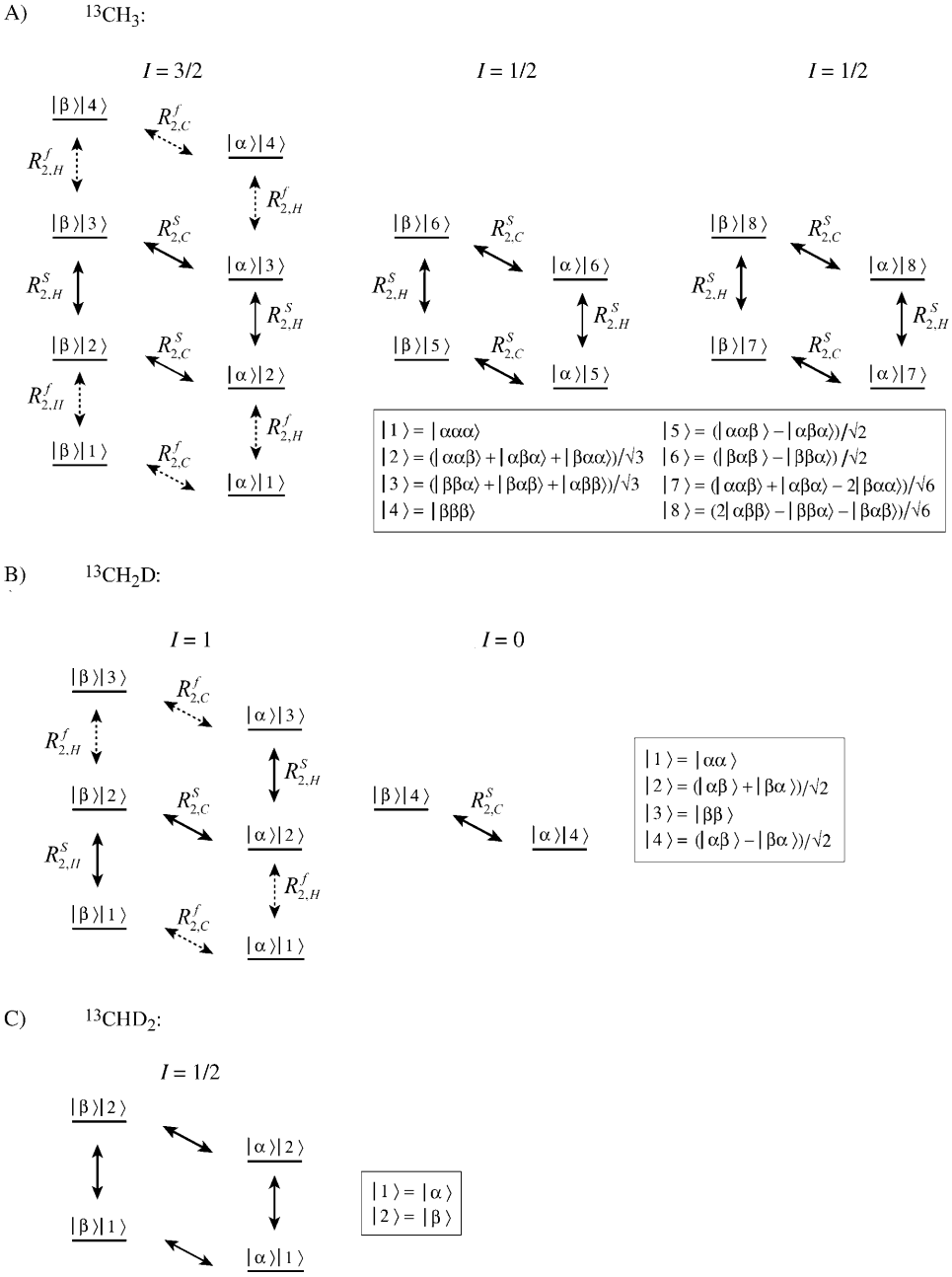

Figure 3. Energy-level diagram for A) $^{13}CH_3$, B) $^{13}CH_2$, and C) ^{13}CH spin systems of rapidly rotating $^{13}CH_3$, $^{13}CH_2D$, and $^{13}CHD_2$ methyl groups. Total spin quantum numbers (I) corresponding to each manifold of $^{13}CH_3$ and $^{13}CH_2$ spin systems are indicated. Slow and fast relaxing ^{13}C/^{1}H transitions are shown with solid and dashed arrows, respectively. A product basis representation of each eigenfunction is used, $|j>|k\rangle$, where $j=\{\alpha,\beta\}$ is the ^{13}C spin state and $k=\{1\text{–}8\}$ is the wave function for the (equivalent) ^{1}H spins.

values for $R^{f}_{2,X}$ are calculated to be 280 and 310 s^{-1}. In the case of $^{13}CHD_2$ methyls, all single-quantum ^1H transitions, and conversely all ^{13}C lines, will relax with the same rates, if cross-correlation effects involving small contributions from chemical-shift anisotropy are neglected. The goal in the design of pulse schemes involving either $^{13}CH_3$ or $^{13}CH_2D$ methyl groups becomes, therefore, to sequester the fast and slowly relaxing transitions in such a way that the observed NMR signal derives from lines that traverse only slowly relaxing pathways. Remarkably, for $^{13}CH_3$ methyl types, the simple HMQC experiment[49,50] is optimal for TROSY "as is", and significant improvements in both sensitivity and resolution in relation to HSQC schemes[51] have been demonstrated on high-molecular-weight proteins.[40] In the case of applications involving studies of methyl dynamics with $^{13}CH_2D$ probes, the methyl-TROSY pulse schemes are more complex, and only become useful for proteins with correlation times in excess of approximately 25 ns, when simpler (HSQC) schemes become particularly inefficient.[41]

Methyl-TROSY, like TROSY involving other spin systems,[52] is sensitive to relaxation contributions from spins other than those of interest,[34] and it is important to minimize such effects. In this regard, a labeling scheme that optimizes the TROSY effect for methyls of Leu and Val has been described that involves protonation of only a single methyl in the isopropyl group, [$^{13}CH_3$,$^{12}CD_3$] by using α-ketoacid precursors **VI** or **VII** (Scheme 1).[53] Residual relaxation contributions from external spins can be minimized by recording zero-quantum (ZQ) methyl-TROSY spectra in which cross-correlated relaxation interactions involving external ^1H and ^2H spins in the protein and methyl ^{13}C and ^1H spins lead to line narrowing.[54] NMR experiments that exploit such effects have been applied in measuring small three-bond methyl ^{13}C, amide ^{15}N *J* couplings in Val side-chains in MSG[55] (see below).

The Role of Methyl Groups in Structural Studies of Large Proteins

The strategy that we have adopted for "structure" determination of high-molecular-weight proteins is somewhat different from that used in analyses of smaller molecules ($\lesssim$ 40 kDa). In studies of "small" proteins, as many ^1H chemical shifts as possible are assigned, and subsequently NOEs connecting large numbers of sites are quantified in terms of distance ranges that are then used to obtain an accurate ensemble of structures.[56] In the case of proteins the size of MSG, it seems unlikely that such an approach will be efficient, since spectral overlap and sensitivity limitations preclude a detailed analysis of all side-chain positions. We prefer, therefore, to focus on key sites in the protein that will provide a sufficient number of restraints to define a backbone global fold for many systems. The global fold then forms the basis for further studies, including additional experiments for refinement of the structure if necessary. It is clear from the above discussion that the probes of choice are methyl groups, along with backbone amides that are assigned during the initial stages of any study. Thus, the goal is to obtain as many methyl–methyl, amide–methyl, and amide–amide NOEs as possible and to supplement the distances derived from them with orientational restraints such as dipolar couplings[57,58] and dihedral angles that are quantified from chemical shifts[59,60] and scalar couplings.[61] Because only a limited subset of the restraints that would normally be obtained in studies of small-to-medium-sized proteins can be measured by using the Ile(δ1), Leu,Val methyl protonation labeling scheme, it is critical that experiments be optimized to take full advantage of the information content that is available.

Once the assignment of methyl groups to specific sites in the protein is completed, stereospecific assignments of the prochiral methyls of Leu and Val can be obtained. For Val residues, a set of quantitative *J*-based experiments[61] for measuring the three-bond methyl-backbone amide ($^3J_{C\gamma N}$) or methyl-carbonyl carbon ($^3J_{C\gamma CO}$) couplings that include the methyl-TROSY effect have been developed and demonstrated on MSG.[55] Figure 4A shows the labeling scheme that has been used for the assignments when only one of the two methyls is $^{13}CH_3$. As we discuss elsewhere in detail, measurement of $^3J_{C\gamma N}$ is best accomplished with a sample prepared with precursor **VII** (Scheme 1) and [D,^{12}C]-glucose (i.e., selective ^{13}C-labeling of only single methyl sites in the protein).[53,55] In contrast, the measurement of $^3J_{C\gamma CO}$ scalar couplings, which requires ^{13}C labeling at both methyl and carbonyl positions, makes use of a sample generated with precursor **VI** and [D,^{13}C]-glucose (the same labeling scheme used for backbone and methyl assignments). Figure 4B illustrates a ZQ-methyl-TROSY quantitative *J* spectrum, recorded for an {Ileδ1($^{13}CH_3$),Leu($^{13}CH_3$,$^{12}CD_3$), Val($^{13}CH_3$,$^{12}CD_3$)} U-[^{15}N,D]-labeled sample of MSG, in which the cross-peak intensities are directly related to the size of $^3J_{C\gamma N}$. A corresponding plot of the methyl-TROSY data set for measuring $^3J_{C\gamma CO}$ is shown in Figure 4C ({Ileδ1($^{13}CH_3$), Leu($^{13}CH_3$,$^{12}CD_3$), Val($^{13}CH_3$,$^{12}CD_3$)} U-[^{15}N,^{13}C,D] sample). Both $^3J_{C\gamma N}$ and $^3J_{C\gamma CO}$ couplings obey Karplus-type relationships that are related to χ_1 torsion angles providing i) stereospecific assignments and ii) χ_1 rotameric states of ordered Val side chains that can be used as dihedral-angle restraints in structure calculations.[61] The information from the measured couplings is complementary to that obtained by using a fractional ^{13}C-labeling technique developed by Neri et al. for stereospecific assignments of Leu,Val methyl groups[62] that was also used in studies of MSG.[55]

The {Ileδ1($^{13}CH_3$),Leu($^{13}CH_3$,$^{12}CD_3$),Val($^{13}CH_3$,$^{12}CD_3$)} U-[^{15}N,D] labeling pattern described above in the context of the measurement of $^3J_{C\gamma N}$ couplings is also particularly useful for recording multidimensional TROSY-based NOE data sets to generate CH_3–CH_3 and HN–CH_3 distances for structural studies (a perdeuterated sample is preferred for HN–HN NOEs). Although the inherent sensitivity of NOESY data sets recorded with Leu/Val ($^{13}CH_3$,$^{12}CD_3$) labeling is lower than when both methyls are of the $^{13}CH_3$ variety, significantly better resolution is obtained in applications in which only one of the isopropyl methyls is protonated, since a major contribution to relaxation is eliminated by removal of the three adjacent protons.[34] In addition, the removal of intraresidue NOE contacts significantly improves the sensitivity of direct NOE correlations and simplifies spectra. Equally important, the elimination of one-bond $^1J_{CC}$ couplings, which would normally be present in fully ^{13}C-labeled proteins, obviates the need for constant time experiments that

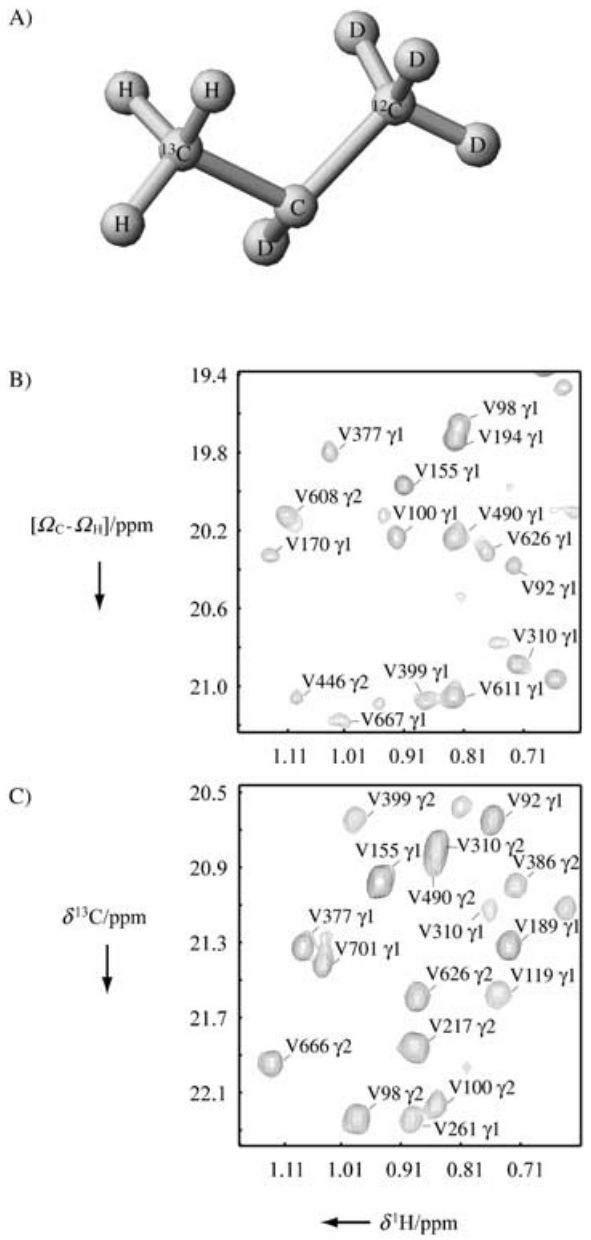

Figure 4. Stereospecific assignments of prochiral methyl carbons of Val side-chains by using methyl-TROSY spectroscopy. A) The labeling scheme that optimizes the methyl-TROSY effect.[53] Only one of the two methyls is $^{13}CH_3$, with the other $^{12}CD_3$; B) Zero-quantum (ZQ) spin echo difference (SED) spectrum recorded on an Ileδ1-[$^{13}CH_3$] Leu,Val-[$^{13}CH_3$,$^{12}CD_3$] U-[D,^{15}N,^{12}C]-labeled MSG sample, 37 °C (D_2O), to quantify $^3J_{C\gamma N}$ coupling constants in Val side chains.[55] The resonances that appear in the spectrum correspond to large (usually $\gtrsim$ 1.5 Hz) $^3J_{C\gamma N}$ couplings. The correlations in the ZQ spectrum appear at frequencies of $(\Omega_C-\Omega_H)$ in the F_1 dimension—here $\Omega_{C,H}$ is the offset from the C,H carrier—and are recast in terms of ^{13}C ppm values; C) Multiple-quantum (MQ) spectrum recorded on an {Ileδ1-[$^{13}CH_3$] Leu,Val-[$^{13}CH_3$,$^{12}CD_3$]} U-[D,^{15}N,^{13}C]-labeled MSG sample, H_2O, for the measurement of $^3J_{C\gamma CO}$ values in Val residues. The resonances that appear in the spectrum correspond to $^3J_{C\gamma CO}$ values larger than approximately 1 Hz. The peaks are labeled with the stereospecific assignments obtained from either the combination of measured $^3J_{C\gamma N}$ and $^3J_{C\gamma CO}$ couplings or the method of fractional (10%) ^{13}C labeling.[55,62]

refocus these couplings at the expense of sensitivity and facilitates the use of potentially longer acquisition times to improve resolution. Recently Konrat and co-workers have found that this labeling scheme is also beneficial for applications involving small proteins.[33]

Figure 5 A, D and E show 2D planes from 4D NOE data sets that form the primary source of distance information in the case of structural studies of MSG.[22,63] In order to optimize both sensitivity and resolution, TROSY versions of the experiments were employed. Consider, for example, the methyl–methyl NOE experiment that provided the majority of the long-range distance constraints in studies of MSG (see below). A methyl-TROSY experiment was developed that exploits the relaxation properties of the long-lived coherences with data recorded by using a nonlinear sampling scheme.[63] In this approach, only approximately 30% of the data that would normally be obtained in a conventional data set is recorded, with data sampling matched to the relaxation profile of the magnetization. In this manner, 4D spectra with excellent resolution can be measured (Figure 5 A, C (upper panel). The high resolution facilitates assignment of the NOE connectivity in Figure 5 A to a Val119γ2–Leu269δ2 contact, despite the fact that the correlation for Leu269δ2 is in a crowded region of the (high-resolution) 2D ^{1}H,^{13}C HMQC map (Figure 5 C, bottom). Constraints involving Val119 are particularly critical because this residue is close to the acetyl-CoA-binding site,[21] and NOE contacts to it (and Val118) are important in defining the central (core) part of the enzyme. The resolution and sensitivity of this 4D data set was similar to the 3D (^{1}H)-^{13}C-^{13}C-H HMQC–NOESY–HMQC and ^{1}H,^{13}C HMQC–NOESY maps recorded on the same sample (Figure 5 B).

A total of 1531 (627 long-range, $|i-j|>3$) approximate distance restraints were assigned from 3D and 4D NOE data sets, supplemented with 415 ^{1}HN–^{15}N dipolar coupling restraints, 300 restraints derived from shifts in ^{13}CO resonance positions upon alignment[64] and 533 (φ,ψ) dihedral-angle restraints based on chemical shifts.[59,60] These restraints were incorporated step-wise in "ab initio" structure calculations.[22] Notably, 85% of the long-range contacts in MSG ($|i-j|>3$) were to methyl groups; this emphasizes the important role of these probes in the determination of global folds of high-molecular-weight proteins.

Figure 6 A compares ribbon backbone representations of the glyoxylate-bound structure of MSG determined by X-ray methods[20] and the solution NMR-derived structure of the apo-form of the enzyme.[22] It is quite clear that the overall structures are very similar and that there are no changes in orientations of the domains upon ligand binding, in contrast to what was predicted on the basis of studies of structurally and functionally related proteins.[65,66] Figure 6 B shows a superposition of the ten lowest energy structures that were derived on the basis of the NMR restraints with the average pair-wise root-mean-squared difference in coordinates of backbone heavy atoms from elements of regular secondary structure indicated (NMR vs. X-ray). Each of the four domains is compared in Figure 6 C–F. Notably, the core domain that is comprised of a triose phosphate isomerase barrel motif[23] with eight parallel β-strands surrounded by eight α-helices is the least well defined. Unlike α-helices, which are well defined through a series of sequential and $i,i\pm3$ amide–amide NOEs, there are far fewer amide con-

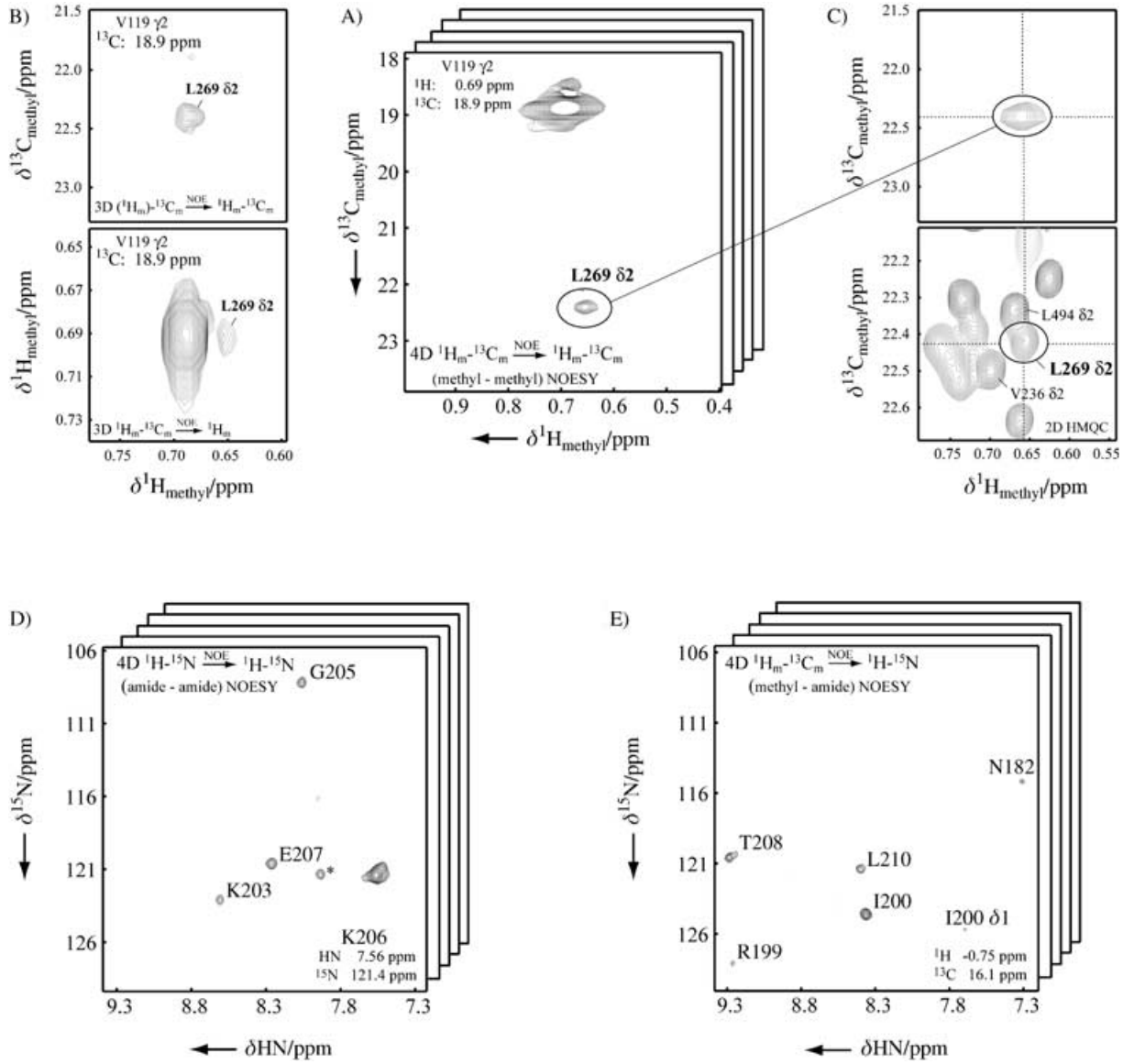

Figure 5. Representative planes from 4D and 3D NOE data sets recorded on samples of MSG: A) $F_1(^1H)$–$F_2(^{13}C)$ plane from the 4D CH_3—CH_3 NOESY spectrum showing correlations to Val119 γ2. The correlation involving Leu269 δ2 can be assigned in spite of the fact that its methyl ^1H,^{13}C chemical shifts place it in a crowded region of the 2D HMQC ^1H,^{13}C correlation map (C, bottom: aliased peaks are in gray). B) top: a region of an $F_1(^{13}C)$–$F_3(^1H)$ plane from the 3D HMQC-NOESY-HMQC at an $F_2(^{13}C)$ frequency of the Val119 γ2 methyl (18.9 ppm) and bottom: a region of the $F_1(^1H)$–$F_3(^1H)$ plane of the 3D HMQC-NOESY, $F_2(^{13}C)$ frequency of 18.9 ppm. D) $F_3(^{15}N)$–$F_4(^1HN)$ plane from the HN—HN 4D data set showing correlations to Lys206 HN. E) $F_3(^{15}N)$–$F_4(^1HN)$ plane from the methyl-HN 4D matrix illustrating NOEs between Ile200 δ1 and proximal amide protons.

nectivities across parallel strands (that are short and twisted). Indeed the labeling strategy that we employ eliminates interstrand NOEs between proximal H_α protons that are most often used to define such elements of secondary structure in the case of fully protonated samples.

MSG is the largest protein (by approximately a factor of two) for which a global NMR fold has been reported. Although the structure is clearly not of high resolution, three of the four domains are within 2 Å of the X-ray coordinates (two within 1.5 Å), and the backbone global fold is within 4 Å of that determined by crystallography.[22] Improvements can be envisioned through the use of data-base approaches, for example.[67–69] However, at the current level of resolution, the relative orientation of domains is well established, and the positions of the active-site residues are reasonably well reproduced. Finally, it is worth mentioning that the frequency of occurrence of Ile/Leu/Val residues in MSG (22%) is essentially that observed in a wide spectrum of proteins (21%), thus it is very likely that global folds of a similar quality to that derived for MSG can be obtained for many other proteins. Indeed, computations that we[8] and others[70] have performed to establish the utility of the approach using a number of different classes of proteins (all α, all β, mixed α+β) suggest that this is indeed the case. Montelione and co-workers advocate the generation of structures from sparse NOE data sets of the type described here as a robust and effective approach for high-throughput analyses of proteins much smaller than MSG.[70]

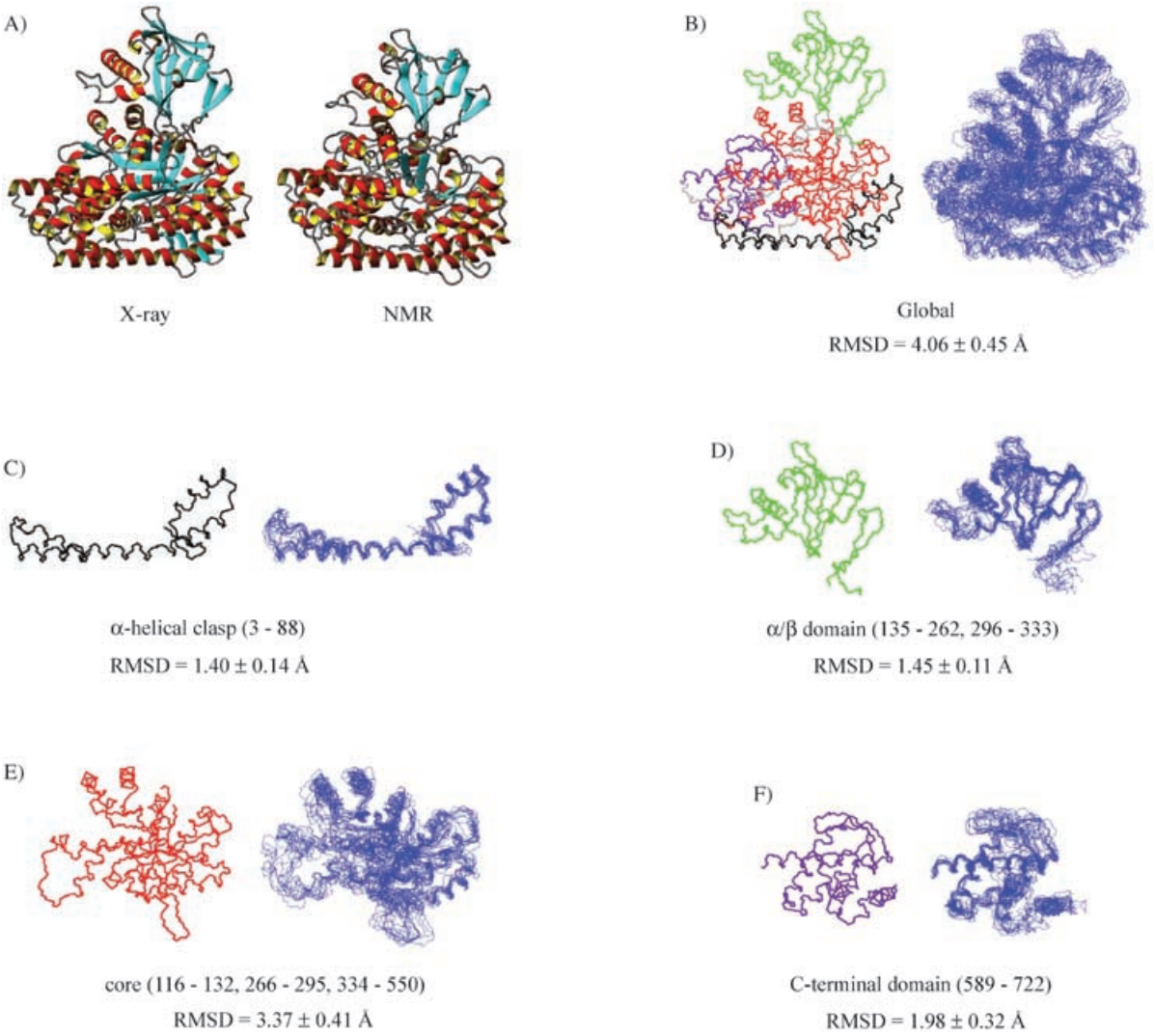

Figure 6. A) Ribbon diagrams of the structure of MSG. Left: X-ray (PDB code 1d8c[20]); right: the lowest-energy NMR structure (PDB code 1y8b[22]) calculated on the basis of 1531 NOE, 1101 dihedral angle, 415 residual dipolar coupling, and 300 carbonyl-shift restraints. B) The X-ray structure of the glyoxylate-bound form of MSG and the ten lowest energy NMR structures of apo-MSG calculated on the basis of experimental restraints. Backbone traces of the X-ray structure (left) and NMR structures (right) are displayed and superimposed by aligning residues in elements of regular secondary structure. Individual domains of MSG: C) α-clasp, D) α/β, E) core and F) C-terminal plug are displayed and superimposed by aligning residues in regular secondary structure. The r.m.s. deviations between the NMR ensemble (10 structures) and the X-ray structure are indicated for heavy backbone atoms of regular secondary structure elements for the entire molecule and for individual domains. Modified from Tugarinov et al.[22]

Methyl Groups as Probes of Side-Chain Dynamics in Proteins

Deuterium has long been incorporated into proteins to simplify the spectra of complex molecules and to improve spectral resolution and sensitivity.[71–73] In these applications, the deuteron is a passive spin; its sole function is to replace protons that have a 6.5-fold larger gyromagnetic ratio, thereby decreasing the relaxation rates of the remaining NMR active spins. The spin properties of the deuteron can be exploited in an active sense as well because it is a wonderful probe of molecular dynamics.[74–77] This derives from the fact that the deuteron is a spin 1 particle and therefore its relaxation and line-shape properties (in the solid state) are dominated by the well understood (and local) quadrupolar interaction.[78] As a result, many applications involving studies of molecular dynamics in the solid state have focused on ^{2}H spin relaxation.[79,80] Over the past decade, a series of experiments involving ^{2}H spin relaxation as a probe of molecular dynamics in proteins in the solution state has been proposed,[12,81] and applications to relatively small proteins have been forthcoming.[82–87] It would clearly be of interest to extend such experiments to higher-molecular-weight proteins. Here, as for smaller proteins, a combination of structural and dynamic studies is needed to properly characterize the molecule. This requires the development of new pulse schemes that take into account the relaxation properties of the probe spin systems.

The initial ^{2}H spin-relaxation experiments focused on methyl groups, since such studies provide a picture of dynamics within the hydrophobic core of a protein.[12] Uniformly ^{13}C-la-

beled proteins with approximately 50% random fractional deuteration were prepared, and the magnetization was transferred from the methyl proton to the deuteron via the intervening carbon, according to $^{1}H \rightarrow {}^{13}C \rightarrow {}^{2}H(T) \rightarrow {}^{13}C(t_1) \rightarrow {}^{1}H(t_2)$, t_1, and t_2 are acquisition times (in these experiments the $^{13}CH_2D$ isotopomer is selected). A series of ^{13}C,^{1}H correlation maps are obtained as a function of T, with the intensity of the correlations related directly to the decay of the deuteron during this interval. These experiments make use of HSQC transfers, and, in the case of a $^{13}CH_2D$ spin system, it can be shown that the carbon lines that are "excited" during the $^{1}H \rightarrow {}^{13}C$ INEPT transfer step above are those that relax rapidly (rates of $R^{f}_{2,C}$, Figure 3B). As a result, the transfer from ^{13}C to ^{2}H is very inefficient in large proteins, and a new scheme must be developed that makes use of the slowly relaxing transitions in $^{13}CH_2D$ spin systems. In this regard, $^{13}CH_2D$-TROSY-based relaxation schemes that are far more sensitive than the original HSQC sequences have recently been proposed for cases in which proteins with correlation times in excess of approximately 25 ns are studied.[41] The sensitivity of the experiments can be significantly further improved by a labeling scheme in which only methyl isotopomers of the $^{13}CH_2D$ variety (Figure 7A, left) are incorporated into the protein so that the methyl of interest has "100% occupancy". In the case of Ile residues, precursor **III** (Scheme 1) is used.

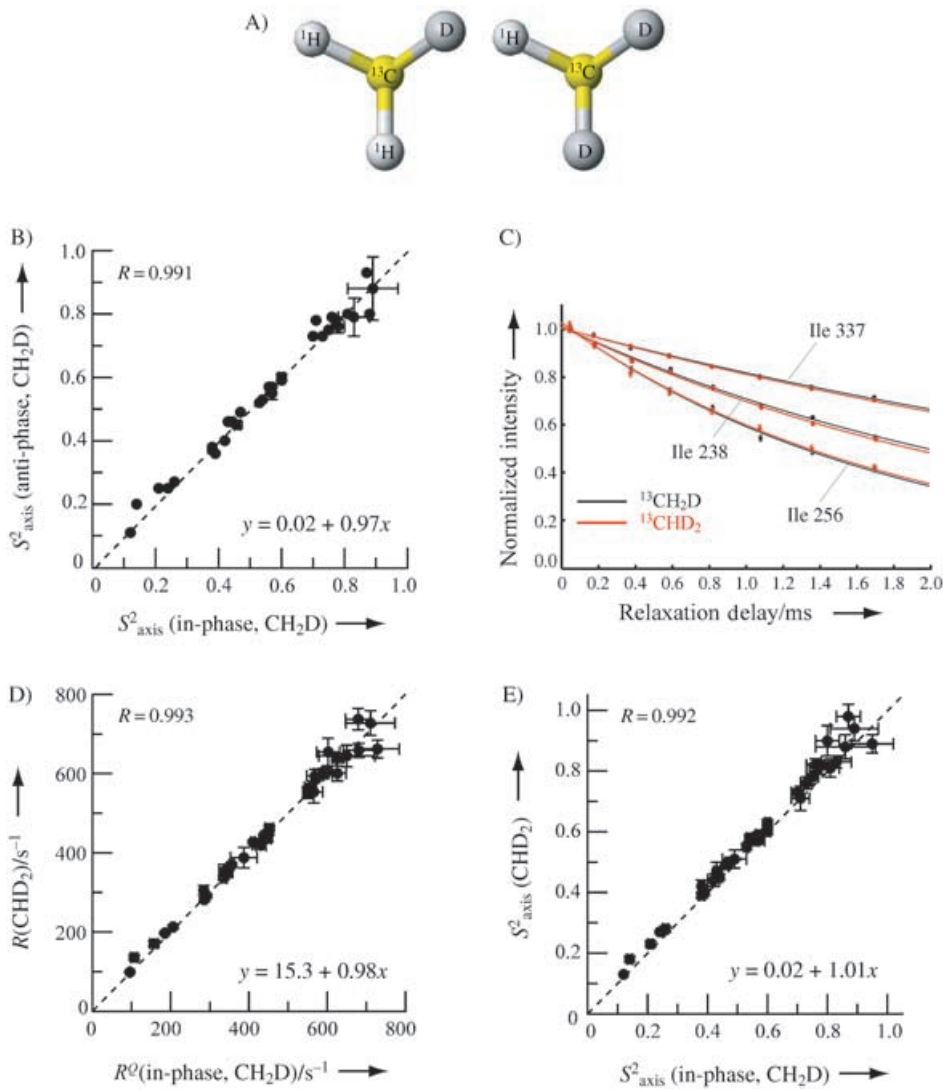

Figure 7. A) Ball-and-stick representation of $^{13}CH_2D$- and $^{13}CHD_2$-labeled methyl groups illustrating the labeling schemes that are used in the study of methyl dynamics via ^{2}H spin relaxation; B) Correlation of S^2_{axis} values derived from relaxation measurements of ^{2}H in-phase and antiphase transverse magnetization; C) Typical relaxation decay curves obtained for several Ileδ1 sites of MSG based on ^{2}H relaxation measurements with $^{13}CH_2D$ (black) and $^{13}CHD_2$ (red) methyls; D) a linear correlation plot of relaxation rates measured on samples with $^{13}CHD_2$ and $^{13}CH_2D$ methyls, $R(^{13}CHD_2)$ (y axis) versus R^{Q}(in-phase,$^{13}CH_2D$) (x axis), respectively; E) $R(^{13}CHD_2)$-derived S^2_{axis} (y axis) versus R^{Q}(in-phase,$^{13}CH_2D$)-derived S^2_{axis} (x axis). Best-fit parameters obtained from linear regression are indicated along with Pearson's correlation coefficients, R.

One of the strengths of the deuteron as a probe of motion is that it is possible to measure the relaxation properties of five unique coherences so that robust measures of dynamics can be extracted.[81,88] Figure 7B shows a correlation between the order parameters squared, S^2_{axis}, defining the amplitude of motion of the (one-bond) C_{methyl}–C axis, measured from the decay of in-phase (x axis) and antiphase (y axis) ^{2}H transverse coherences in Ile $^{13}CH_2D$ methyl groups of MSG. The excellent agreement between the two measures is readily apparent. For applications involving large proteins, it is also possible to measure dynamics by using $^{13}CHD_2$ isotopomers (Figure 7A, right), and theory predicts that the rates of transverse relaxation of the deuteron(s) in $^{13}CH_2D$ and $^{13}CHD_2$ methyls should be very similar.[41] Figure 7C, D shows that this is indeed the case. Values of S^2_{axis} extracted from studies of $^{13}CH_2D$ (x axis) and $^{13}CHD_2$ groups (y axis; Figure 7E) are highly correlated.[41] The small offset of approximately 0.03 in S^2_{axis} between the two probes likely reflects errors in estimation of the overall molecular tumbling times in the two separate samples that is needed for the calculation of order parameters.

Concluding Remarks

In this review, we have briefly highlighted a number of applications of methyl groups as probes of molecular structure and

dynamics in the 82 kDa enzyme malate synthase G. Central to this work has been the development of NMR experiments that exploit the isotope-labeling schemes that produce highly deuterated, methyl protonated proteins and the fact that samples with different methyl labeling patterns ($^{13}CH_3$, $^{13}CD_3$, $^{13}CHD_2$, $^{13}CH_2D$) can be prepared quantitatively for a variety of applications. The large number of sample permutations that is now possible can make it confusing for the nonexpert to know what type of labeling scheme to use and, indeed, the optimal approach for one system might not be suitable for another. Nevertheless, it is worth summarizing what we feel are the most useful samples for both structural and dynamic studies at least for the case of MSG. Assignments of backbone nuclei (and $^{13}C_\beta$ carbons) as well as Ile(δ1), Leu, and Val methyl groups can be accomplished by using an {Ileδ1-($^{13}CH_3$),Leu($^{13}CH_3$,$^{12}CD_3$),Val($^{13}CH_3$,$^{12}CD_3$)} U-[^{15}N,^{13}C,D] sample in H_2O[89] that can also be used for the measurement of $^3J_{C\gamma CO}$ couplings[55] and HN–CH_3, HN–HN NOEs[22] (although we prefer a perdeuterated sample for obtaining amide–amide distance restraints). A second sample in D_2O with the methyl labeling scheme as above but in which all other carbon positions are ^{12}C ({Ileδ1($^{13}CH_3$),Leu($^{13}CH_3$,$^{12}CD_3$),Val($^{13}CH_3$,$^{12}CD_3$)} U-[^{15}N,^{12}C,D]) facilitates optimal measurement of $^3J_{C\gamma N}$ couplings[55] as well as CH_3–CH_3 NOEs.[22,63] The latter sample can also be used for studies of methyl dynamics on the ms timescale,[90] while studies of ps–ns timescale motions at methyl positions by using ^{2}H spin relaxation are performed on samples with either $^{13}CH_2D$ or $^{13}CHD_2$ methyls.[41] The interested reader is referred to the original literature cited above for a detailed breakdown of measurement time for each experiment. The results summarized in this review on MSG establish that quantitative information of the sort that has normally been generated only in NMR studies of small-to-moderately sized proteins can also be obtained, at least in some cases, in applications involving molecules in the 100 kDa molecular weight range.

Acknowledgements

This work was supported by a grant from the Canadian Institutes of Health Research (CIHR) to L.E.K. We thank Dr. W.-Y. Choy (University of Western Ontario, Canada) for the preparation of Figure 6. L.E.K. holds a Canada Research Chair in Biochemistry.

Keywords: global protein fold · high-molecular-weight proteins · isotopic labeling · malate synthase G · methyl isotopomer · methyl-TROSY · NMR spectroscopy · side-chain dynamics

[1] J. Janin, S. Miller, C. Chothia, *J. Mol. Biol.* **1988**, *204*, 155.
[2] L. K. Nicholson, L. E. Kay, D. M. Baldisseri, J. Arango, P. E. Young, A. Bax, D. A. Torchia, *Biochemistry* **1992**, *31*, 5253.
[3] V. Tugarinov, P. M. Hwang, L. E. Kay, *Annu. Rev. Biochem.* **2004**, *73*, 107.
[4] M. K. Rosen, K. H. Gardner, R. C. Willis, W. E. Parris, T. Pawson, L. E. Kay, *J. Mol. Biol.* **1996**, *263*, 627.
[5] W. J. Metzler, M. Wittekind, V. Goldfarb, L. Mueller, B. T. Farmer, *J. Am. Chem. Soc.* **1996**, *118*, 6800.
[6] B. O. Smith, Y. Ito, A. Raine, S. Teichmann, L. Ben-Tovim, D. Nietlispach, R. W. Broadhurst, T. Terada, M. Kelly, K. Oschkinat, T. Shibata, S. Yokoyama, E. D. Laue, *J. Biomol. NMR* **1996**, *8*, 360.
[7] K. H. Gardner, M. K. Rosen, L. E. Kay, *Biochemistry* **1997**, *36*, 1389.
[8] G. A. Mueller, W. Y. Choy, D. Yang, J. D. Forman-Kay, R. A. Venters, L. E. Kay, *J. Mol. Biol.* **2000**, *300*, 197.
[9] P. J. Hajduk, D. J. Augeri, J. Mack, R. Mendoza, J. G. Yang, S. F. Betz, S. W. Fesik, *J. Am. Chem. Soc.* **2000**, *122*, 7898.
[10] J. D. Gross, V. M. Gelev, G. Wagner, *J. Biomol. NMR* **2003**, 235.
[11] G. D. Henry, J. H. Weiner, B. D. Sykes, *Biochemistry* **1986**, *25*, 590.
[12] D. R. Muhandiram, T. Yamazaki, B. D. Sykes, L. E. Kay, *J. Am. Chem. Soc.* **1995**, *117*, 11536.
[13] R. Ishima, J. M. Louis, D. A. Torchia, *J. Am. Chem. Soc.* **1999**, *121*, 11589.
[14] A. L. Lee, A. J. Wand, *Nature* **2001**, *411*, 501.
[15] N. R. Skrynnikov, F. A. A. Mulder, B. Hon, F. W. Dahlquist, L. E. Kay, *J. Am. Chem. Soc.* **2001**, *123*, 4556.
[16] F. A. A. Mulder, A. Mittermaier, B. Hon, F. W. Dahlquist, L. E. Kay, *Nat. Struct. Biol.* **2001**, *8*, 932.
[17] W. Y. Choy, D. Shortle, L. E. Kay, *J. Am. Chem. Soc.* **2003**, *125*, 1748.
[18] Z. Serber, W. Straub, L. Corsini, A. M. Nomura, N. Shimba, C. S. Craik, P. Ortiz de Montellano, V. Dötsch, *J. Am. Chem. Soc.* **2004**, *126*, 7119.
[19] I. Molina, M. T. Pellicer, J. Badia, J. Aguilar, L. Baldoma, *Eur. J. Biochem.* **1994**, *224*, 541.
[20] B. R. Howard, J. A. Endrizzi, S. J. Remington, *Biochemistry* **2000**, *39*, 3156.
[21] D. M. Anstrom, K. Kallio, S. J. Remington, *Protein Sci.* **2003**, *12*, 1822.
[22] V. Tugarinov, W. Y. Choy, V. Y. Orekhov, L. E. Kay, *Proc. Natl. Acad. Sci. USA* **2005**, *102*, 622.
[23] D. Voet, J. G. Voet, *Biochemistry*, 3rd ed., Wiley, New York, **2004**.
[24] W. Bishai, *Nature* **2000**, *406*, 683.
[25] M. C. Lorentz, G. R. Fink, *Nature* **2001**, *412*, 83.
[26] C. V. Smith, C. Huang, A. Miczak, D. G. Russell, J. C. Sacchettini, K. Honer zu Bentrup, *J. Biol. Chem.* **2003**, *278*, 1735.
[27] M. K. Rosen, K. H. Gardner, R. C. Willis, W. E. Parris, T. Pawson, L. E. Kay, *J. Mol. Biol.* **1996**, *263*, 627.
[28] A. L. Lee, J. L. Urbauer, A. J. Wand, *J. Biomol. NMR* **1997**, *9*, 437.
[29] R. Ishima, J. M. Louis, D. A. Torchia, *J. Mol. Biol.* **2001**, *305*, 515.
[30] K. H. Gardner, L. E. Kay, *J. Am. Chem. Soc.* **1997**, *119*, 7599.
[31] N. K. Goto, K. H. Gardner, G. A. Mueller, R. C. Willis, L. E. Kay, *J. Biomol. NMR* **1999**, *13*, 369.
[32] K. H. Gardner, X. Zhang, K. Gehring, L. E. Kay, *J. Am. Chem. Soc.* **1998**, *120*, 11738.
[33] R. Lichtenecker, M. L. Ludwiczek, W. Schmid, R. Konrat, *J. Am. Chem. Soc.* **2004**, *126*, 5348.
[34] V. Tugarinov, L. E. Kay, *J. Am. Chem. Soc.* **2003**, *125*, 13868.
[35] V. Tugarinov, L. E. Kay, *J. Am. Chem. Soc.* **2003**, *125*, 5701.
[36] L. G. Werbelow, D. M. Grant, *Adv. Magn. Reson.* **1977**, *9*, 189.
[37] R. L. Vold, R. R. Vold, *Prog. Nucl. Magn. Reson. Spectrosc.* **1978**, *12*, 79.
[38] K. Pervushin, R. Riek, G. Wider, K. Wüthrich, *Proc. Natl. Acad. Sci. USA* **1997**, *94*, 12366.
[39] K. Pervushin, R. Riek, G. Wider, K. Wüthrich, *J. Am. Chem. Soc.* **1998**, *120*, 6394.
[40] V. Tugarinov, P. M. Hwang, J. E. Ollerenshaw, L. E. Kay, *J. Am. Chem. Soc.* **2003**, *125*, 10420.
[41] V. Tugarinov, J. E. Ollerenshaw, L. E. Kay, *J. Am. Chem. Soc.* **2005**, 127, 8214.
[42] E. Miclet, D. C. Williams, Jr, G. M. Clore, D. L. Bryce, J. Boisbouvier, A. Bax, *J. Am. Chem. Soc.* **2004**, *126*, 10560.
[43] L. G. Werbelow, A. G. Marshall, *J. Magn. Reson.* **1973**, 299.
[44] L. E. Kay, J. H. Prestegard, *J. Am. Chem. Soc.* **1987**, *109*, 3829.
[45] N. Müller, G. Bodenhausen, R. R. Ernst, *J. Magn. Reson.* **1987**, *75*, 297.
[46] L. E. Kay, T. E. Bull, *J. Magn. Reson.* **1992**, *99*, 615.
[47] L. E. Kay, D. A. Torchia, *J. Magn. Reson.* **1991**, *95*, 536.
[48] J. H. Prestegard, D. M. Grant, *J. Am. Chem. Soc.* **1978**, *100*, 4664.
[49] L. Mueller, *J. Am. Chem. Soc.* **1979**, *101*, 4481.
[50] A. Bax, R. H. Griffey, B. L. Hawkings, *J. Magn. Reson.* **1983**, *55*, 301.
[51] G. Bodenhausen, D. J. Rubin, *Chem. Phys. Lett.* **1980**, *69*, 185.
[52] M. Salzmann, K. Pervushin, G. Wider, H. Senn, K. Wüthrich, *Proc. Natl. Acad. Sci. USA* **1998**, *95*, 13585.
[53] V. Tugarinov, L. E. Kay, *J. Biomol. NMR* **2004**, *28*, 165.
[54] V. Tugarinov, R. Sprangers, L. E. Kay, *J. Am. Chem. Soc.* **2004**, *126*, 4921.
[55] V. Tugarinov, L. E. Kay, *J. Am. Chem. Soc.* **2004**, *126*, 9827.

[56] K. Wüthrich, *NMR of Proteins and Nucleic Acids*, Wiley, New York, **1986**.
[57] J. R. Tolman, J. M. Flanagan, M. A. Kennedy, J. H. Prestegard, *Proc. Natl. Acad. Sci. USA* **1995**, *92*, 9279.
[58] N. Tjandra, A. Bax, *Science* **1997**, *278*, 1111.
[59] G. Cornilescu, F. Delaglio, A. Bax, *J. Biomol. NMR* **1999**, *13*, 289.
[60] D. S. Wishart, B. D. Sykes, *J. Biomol. NMR* **1994**, *4*, 171.
[61] A. Bax, G. W. Vuister, S. Grzesiek, F. Delaglio, A. C. Wang, R. Tschudin, G. Zhu, *Methods Enzymol.* **1994**, *239*, 79.
[62] D. Neri, T. Szyperski, G. Otting, H. Senn, K. Wüthrich, *Biochemistry* **1989**, *28*, 7510.
[63] V. Tugarinov, L. E. Kay, I. Ibraghimov, V. Y. Orekhov, *J. Am. Chem. Soc.* **2005**, *127*, 2767.
[64] G. Cornilescu, J. Marquardt, M. Ottiger, A. Bax, *J. Am. Chem. Soc.* **1998**, *120*, 6836.
[65] T. M. Larsen, L. T. Laughlin, H. M. Holden, I. Rayment, G. H. Reed, *Arch. Biochem. Biophys.* **1997**, *345*, 199.
[66] S. J. Remington, G. Wiegand, R. Huber, *J. Mol. Biol.* **1982**, *158*, 111.
[67] C. A. Rohl, C. E. Strauss, K. M. Misura, D. Baker, *Methods Enzymol.* **2004**, *383*, 66.
[68] J. L. Mueller, D. R. Ripoll, C. F. Aquadro, M. F. Wolfner, *Proc. Natl. Acad. Sci. USA* **2004**, *101*, 13 542.
[69] A. R. Leach, *Molecular Modelling. Principles and Applications*, 2nd ed., Prentice Hall, Dorchester, **2001**.
[70] D. Zheng, Y. J. Huang, H. N. Moseley, R. Xiao, J. Aramini, G. V. Swapna, G. T. Montelione, *Protein Sci.* **2003**, *12*, 1232.
[71] H. L. Crespi, R. M. Rosenberg, J. J. Katz, *Science* **1968**, *161*, 795.
[72] J. L. Markley, I. Putter, O. Jardetzky, *Science* **1968**, *161*, 1249.
[73] D. M. LeMaster, *Q. Rev. Biophys.* **1990**, *23*, 133.
[74] L. W. Jelinski, C. E. Sullivan, D. A. Torchia, *Nature* **1980**, *284*.
[75] J. Seelig, *Q. Rev. Biophys.* **1977**, *10*, 353.
[76] M. A. Keniry, T. M. Rothgeb, R. L. Smith, H. S. Gutowsky, E. Oldfield, *Biochemistry* **1983**, *22*, 1917.
[77] R. R. Vold, R. L. Vold, *Adv. Magn. Opt. Reson.* **1991**, *16*, 85.
[78] A. Abragam, *Principles of Nuclear Magnetism*, Clarendon, Oxford, **1961**.
[79] S. Vega, A. Pines, *J. Chem. Phys.* **1977**, *66*, 5624.
[80] R. Tycko, *Nuclear Magnetic Resonance Probes of Molecular Dynamics*, Kluwer, Boston, **1994**.
[81] O. Millet, D. R. Muhandiram, N. R. Skrynnikov, L. E. Kay, *J. Am. Chem. Soc.* **2002**, *124*, 6439.
[82] D. Yang, A. Mittermaier, Y. K. Mok, L. E. Kay, *J. Mol. Biol.* **1998**, *276*, 939.
[83] A. L. Lee, P. F. Flynn, A. J. Wand, *J. Am. Chem. Soc.* **1999**, *121*, 2891.
[84] R. Ishima, A. P. Petkova, J. M. Louis, D. A. Torchia, *J. Am. Chem. Soc.* **2001**, *123*, 6164.
[85] O. Millet, A. Mittermaier, D. Baker, L. E. Kay, *J. Mol. Biol.* **2003**, *329*, 551.
[86] E. C. Johnson, T. M. Handel, *J. Biomol. NMR* **1999**, *15*, 135.
[87] R. B. Best, T. J. Rutherford, S. M. Freund, J. Clarke, *Biochemistry* **2004**, *43*, 1145.
[88] N. R. Skrynnikov, O. Millet, L. E. Kay, *J. Am. Chem. Soc.* **2002**, *124*, 6449.
[89] V. Tugarinov, R. Muhandiram, A. Ayed, L. E. Kay, *J. Am. Chem. Soc.* **2002**, *124*, 10 025.
[90] D. M. Korzhnev, K. Kloiber, V. Kanelis, V. Tugarinov, L. E. Kay, *J. Am. Chem. Soc.* **2004**, *126*, 3964.

Received: March 18, 2005
Published online on August 1, 2005

